n-Type Field Effect Transistors Based on Rigid Rod and Liquid Crystalline Alternating Copoly(benzobisoxazole) Imides Containing Perylene and/or Naphthalene

ARTICLE *in* THE JOURNAL OF PHYSICAL CHEMISTRY B · DECEMBER 2010

Impact Factor: 3.3 · DOI: 10.1021/jp107232u · Source: PubMed

4 AUTHORS, INCLUDING:

Nagesh Kolhe
CSIR - National Chemical Laboratory, Pune
5 PUBLICATIONS **54** CITATIONS
SEE PROFILE

Asha S. K
CSIR - National Chemical Laboratory, Pune
53 PUBLICATIONS **584** CITATIONS
SEE PROFILE

Ks Narayan
Jawaharlal Nehru Centre for Advanced Sci…
154 PUBLICATIONS **1,725** CITATIONS
SEE PROFILE

n-Type Field Effect Transistors Based on Rigid Rod and Liquid Crystalline Alternating Copoly(benzobisoxazole) Imides Containing Perylene and/or Naphthalene

Nagesh B. Kolhe,[†] S. K. Asha,*[,†] Satyaprasad P. Senanayak,[‡] and K. S. Narayan*[,‡]

Polymer Science & Engineering Division, National Chemical Laboratory, Pune-411008, Maharashtra, India, and Jawaharlal Nehru Centre for Advanced Scientific Research, Jakur, Bangalore 560064, Karnataka, India

Received: August 2, 2010; Revised Manuscript Received: October 26, 2010

The synthesis, characterization, and device studies of poly(benzobisoxazole imide)s containing perylene or naphthalene units in an alternating fashion with the oxazole unit are described. Photoinduced energy transfer and charge separation were studied in methanesulfonic acid (MSA) solution via absorption, excitation, and steady-state fluorescence studies. Excitation of the bisoxazole moiety resulted in enhanced emission from the perylene bisimide unit as a result of FRET (Förster resonance energy transfer). The influence of the imide substitution into the linear chain of poly(benzobisoxazole) (PBO) on its solid-state packing was examined by wide-angle X-ray diffraction (WXRD) analysis. Bottom contact field effect transistors (FET) based on thermally annealed polymer films were fabricated and studied. The polymers showed n-type charge transport and current modulation with an on/off ratio greater than 10^2. It was observed that the FETs consisting of the random copolymer of bisoxazole containing both perylene as well as naphthalene bisimide units had higher performance parameters such as better mobility (μ_e) and I_{on}/I_{off} ratio compared to those of the pristine systems.

Introduction

Poly(benzobisoxazole)s (PBOs) belong to the heterocyclic rigid-rod π-conjugated polymer family which exhibits high tensile strength, high modulus, and excellent thermal and environmental stability due to the high degree of intermolecular $\pi-\pi$ interactions present in the solid state.[1−5] In addition to these, they have been shown to have excellent electron transport properties. Pioneering work has been done on poly(benzobisthiazole)s and poly(benzobisoxazole)s by the group of Jenekhe et al.[6−8] They copolymerized the rigid rod π-conjugated bisazoles with various electron rich systems, such as phenylenevinylene or thiophene, and reported Organic Light Emitting Diodes (OLEDS) as well as bulk heterojunction solar cell devices based on them.[6,8] Aromatic polyimides are also a class of high performance polymers that have gained considerable attention in microelectronics, aerospace, and photoelectronics because of their excellent thermal stability, moisture resistance, mechanical strength, and electrical properties. There are examples in literature where the properties of polyimides have been improved by incorporation with ether, amide, or ester functional groups.[9,10] The properties that are not attainable in a single polymer can most often be realized by copolymerization of the respective monomers to obtain new polymers exhibiting good properties of both the parent homopolymers. Poly(oxazole imide)s can be prepared by the reaction of diamines containing preformed benzoxazole moieties with dianhydrides. Combining the imide and oxazole moiety together in poly(benzoxazole imide)s gives rise to a new class of rigid rod polymers having advantageous characteristics of both systems and which can fall in the niche category of n-type materials.[11−14] Substantial progress has been made in developing p-type conjugated polymers where mobility as high as $\approx$0.1 cm^2 V^{-1} s^{-1} have been observed.[15,16] Comparatively development of polymers with high electron mobility has not been so active except for a recent flurry of activity in the last couple of years.[17,18] Exploration of new polymer semiconductors that have good air and thermal stability are important for device applications. In this context, design of new materials based on PBO and bisimides of perylene or naphthalene can provide structures with high mechanical strength and reasonable electron mobility.

Processing in both these rigid aromatic systems is done through precursors which are soluble. For instance in polyimides, thermal imidization of the precursor poly(amic acid) results in films of polyimide.[12,13] In the PBO system also the precursor poly(*o*-hydroxy amide) derived from the polycondenzation of diacid derivative with bis(*o*-aminophenol) is soluble and thermal cyclodehydration to film is possible.[19] But Jenekhe et al. have standardized a procedure for developing large area films of PBO type of polymers that can be made use for photovoltaic applications. It consists of formation of reversible Lewis acid coordination complexes by preparing isotropic solutions of the rigid rod poly(benzobisoxazole)s in nitromethane containing aluminum chloride ($AlCl_3$) or galium chloride ($GaCl_3$).[20,21] This polymer−Lewis acid complex is coated on the required substrate and then washed several times with deionized water and subsequently left in deionized water overnight to ensure complete removal of the Lewis acid. Finally, the polymer thin films are dried for 6 h at 80 °C in a vacuum oven. Another advantageous property of the PBO system which could be exploited in their copolymers is their ability to be spun into fibers from ordered lyotropic phases in solvents such as PPA.[1,5] Although the liquid crystal phase is short-range ordered, induced alignment of the self-organized polymer under an external force can increase the degree of orientational order over a substantially longer range in the desired direction.

Perylene and naphthalene bisimides are important n-type semiconducting materials that find application in photovoltaics, light emitting diodes, field effect transistors, etc., because of their relative high electron affinity.[22−30] Perylene bisimides exhibit intense fluorescence with quantum yield reaching nearly

* Corresponding authors. (S.K.A.) E-mail: sk.asha@ncl.res.in. Fax: 0091-20-25902615. (K.S.N.) E-mail: narayan@jncasr.ac.in.
[†] National Chemical Laboratory.
[‡] Jawaharlal Nehru Centre for Advanced Scientific Research.

10.1021/jp107232u
Published on Web 11/23/2010

unity. This article describes the synthesis, structural characterization, and photophysical as well as charge transport characteristics of poly(benzoxazole imides) based on perylene and naphthalene bisimides in a solution in methanesulfonic acid (MSA) as well as in film. Exactly alternating perylene bisimide−bisoxazole and naphthalene bisimide−bisoxazole copolymers as well as a random copolymer incorporating both perylene and naphthalene bisimide units alternating with bisoxazole units were synthesized and characterized. The photoinduced energy transfer and charge separation was studied in methanesulfonic acid (MSA) solution via absorption, excitation, and steady-state fluorescence studies. Unlike the substantial work on copolymer and blend (p) donor systems where energy transfer has been demonstrated,[31] there are not many reports on energy transfer in (n) acceptor copolymer systems. The lyotropic liquid crystalline characteristics in MSA as well as the transport characteristics in the form of thin films in organic field effect transistor (OFET) devices of these novel copolymers were also studied. We also demonstrate the degree of thermal stability in these systems where the performance increases with thermal treatment. Both the poly(benzobisoxazole)s and bisimides have been shown to develop improved ordering upon subjecting to heat treatment.[30,32] X-ray diffraction studies have shown a structural ordering occurring upon annealing PBO fibers and energy calculations have been performed, supporting this phenomenon of regularization of randomly distributed chains to more restricted chains following heat treatment.[31,32] This ability was taken to good advantage in copolymers based on both the systems reported here. Dramatic improvement in the FET device characteristics were observed upon annealing to 150−160 °C.[28,33] The reasonably good n-type performance and electron transport mobilities of these new poly(benzoxazole imides) suggested that these are promising materials for processable high-performance applications.

Experimental Section

Materials. 2,4-Diamino-1,5-benzenediol dihydrochloride (DADHB), terephthalic acid polyphosphoric acid 83% (PPA), 4-aminobenzoic acid, perylene-3,4,9,10-tetracarboxylic dianhydride (PTCDA), isoquinoline, 1,4,5,8-naphthalenetetracarboxy dianhydride (NTCDA), and methanesulfonic acid were purchased from Sigma-Aldrich. PTCDA was purified using the reported procedure.[28] NTCDA was purified using sublimation, and *m*-cresol was purchased locally and vacuum distilled twice before polymerization.

Measurements. ^{1}H NMR and solid-state ^{13}CNMR spectra were recorded using 400-MHz Bruker NMR spectrophotometer in $D_2SO_4 + D_2O$ containing small amounts of TMS as internal standard. Infrared spectra were recorded using a Perkin-Elmer Spectrum one FT-IR spectrophotometer in the range of 4000 to 400 cm^{-1}. UV−vis spectra were recorded using a Perkin-Elmer Lambda 950 UV−vis spectrometer. Steady-state fluorescence, excitation, and emission measurements were performed using a Fluorolog Horiba Jobin Yvon fluorescence spectrophotometer. The fluorescence quantum yields of the polymer and model compounds (for perylene) were determined in MSA using Rhodamine 6G in water ($\phi = 0.95$) as the standard by exciting at 510 nm. The quantum yields for bisoxazole (quenched emission) were determined in MSA using anthracene in cyclohexane ($\phi = 0.36$) as standard by exciting at 343 nm whereas for the homopolymer (PBO) they were determined in MSA using quinine sulfate in 0.1 N H_2SO_4 ($\phi = 0.54$) as the standard by exciting at 350 nm. All the solutions were prepared having 0.1 OD at the exciting wavelength. Thermogravimetric analysis (TGA) was performed using a Perkin-Elmer Thermo gravimetric Analyzer. Samples were run from 30 to 800 °C with a heating rate of 10 °C/min under nitrogen. The phase behaviors of the molecules were analyzed using a polarized light microscope (Leitz-1350). WAXRD were recorded using Phillips x'pertpro powder X-ray diffractometer using Cu Kα radiation, and the spectra were recorded in the range of $2\theta = 3-50°$ and at 2° per minute. Electrochemical behavior of model compounds and copolymers were studied by using a BAS-Epsilon potentiostat. The inherent viscosities were measured with an ubbelodhe viscometer at 30 ± 0.1 °C in methanesulfonic acid at a concentration of 0.5 g/dL. Scanning electron microscopy (SEM) images were obtained with an FEI system (Model, Quanta 200 3D Dual beam SEM with EDAX) with a tungsten filament as electron source.

Device Fabrication. Bottom-contact, top-gate and top-contact, bottom-gate structures were fabricated for field effect transistor studies. Consistent, reproducible, enhanced, and leakage-free performance were obtained more reliably for the bottom-contact, top-gate geometry. The fabrication procedure involved an initial thin film semiconductor layer spin-coated under ambient conditions from a 12 mg/mL solution in methanesulfonic acid (MSA) of PBO and copolymers PerPBO, NapPBO, and NapPerPBO at 1000 rpm for 1 min on hexamethyldisilizane (HMDS)-treated glass substrates. Prior to deposition, the glass substrates were cleaned as per the standard procedure of RCA treatment. HMDS treatment of the glass substrate was done by spin-coating of HMDS in liquid at 1500 rpm for 30 s and heating the substrates at 110 °C for 2 h. After the spin-coating of the semiconducting layer from the MSA solution, the resulting films were treated with methanol for about 30 min and then in deionized water for 10−12 h to remove any traces of MSA. All the devices were then dried in vacuum for 10−12 h at 70 °C to remove traces of water. Then the semiconducting films were annealed at 150−160 °C for 30 min in a glovebox. This was followed by vapor deposition of Al electrodes (10^{-6} mbar, 1 Å^0/s, 40 nm thick) onto the semiconducting film through a shadow mask to obtain channels of 60−80 μm length and 1−2 mm width. It was observed that Al formed better injecting contacts compared to Au electrodes. This is due to the fact that the LUMO level of these model polymers and monomers lie closer to the Fermi level of Al as compared to that of Au; hence, these polymers form a blocking contact with Au. After the electrode deposition, a dielectric bilayer of polyvinylidene fluoride (PVDF) and polyvinyl alcohol (PVA) were coated. The PVDF film was coated from a 60 mg/mL solution in *N*,*N*-dimethylacetamide at 1000 rpm for 1 min giving a film of thickness 350 nm (capacitance per unit area 15 nF/cm^2). The film was rapidly annealed at 150 °C in vacuum to facilitate the formation of a uniform β-phase. This was followed by a buffer layer of PVA coated from a 20 mg/mL solution in deionized water at 1000 rpm for 30 s (capacitance per unit area ~10 nF/cm^2). The film was then dried in vacuum at 70 °C for 10−12 h to remove traces of water. The Al gate electrode was vapor-deposited (10^{-6} mbar, 0.1 Å^0/s, 40 nm thick). The bilayer of dielectric thus formed consisting of PVDF and PVA had effective capacitance C_0 in the range of 6−8 nF/cm^2 measured directly using a Keithley 4200 semiconductor parameter analyzer for a film of thickness ~450 nm. The electrical characterization of the transistor devices was performed with two identical source meters, the Keithley 2400 and the high impedance electrometer Keithley 6514, and cross-checked with measurements from a standard Keithley 4200 semiconductor parameter analyzer. The mobility values are reported as the median values for measure-

SCHEME 1: Synthesis of Homo- and Copolymers

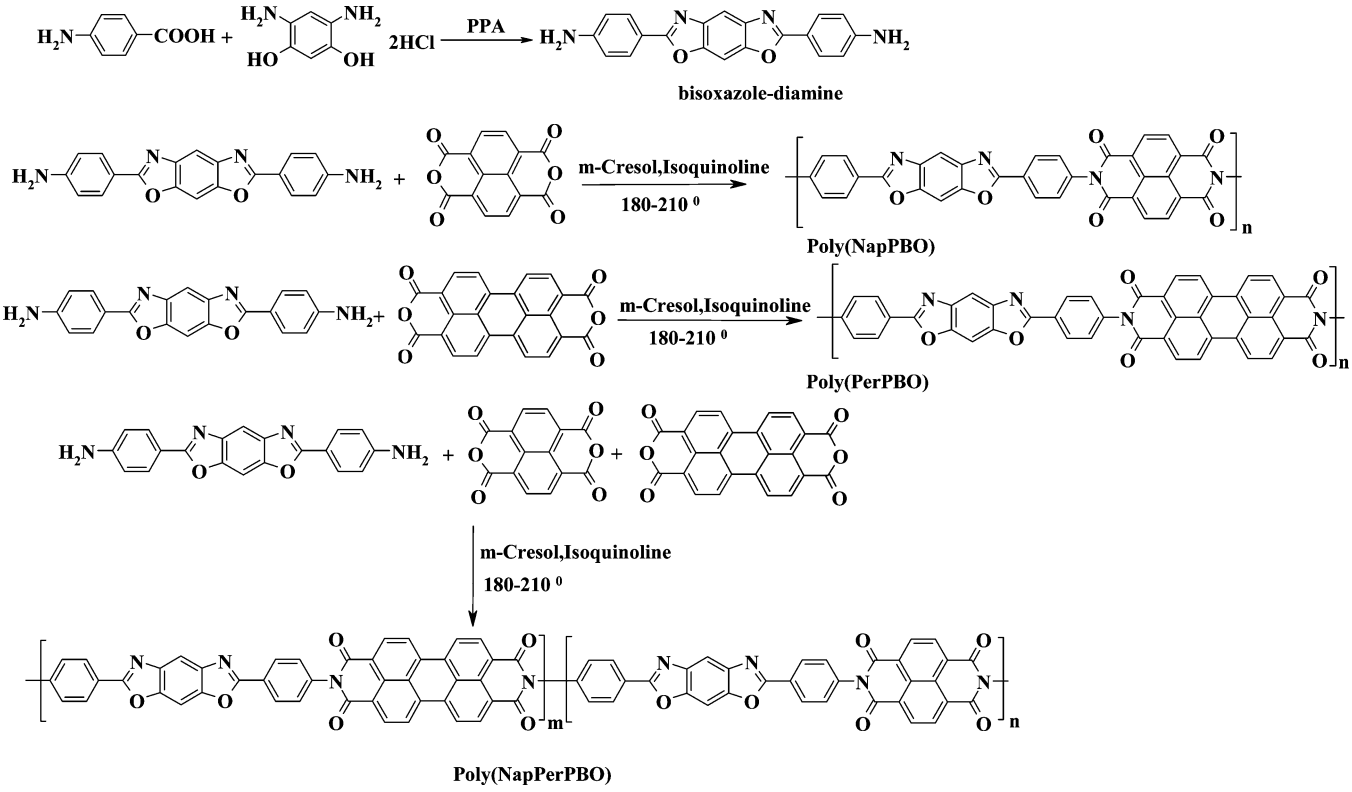

SCHEME 2: Synthesis of Model Compounds

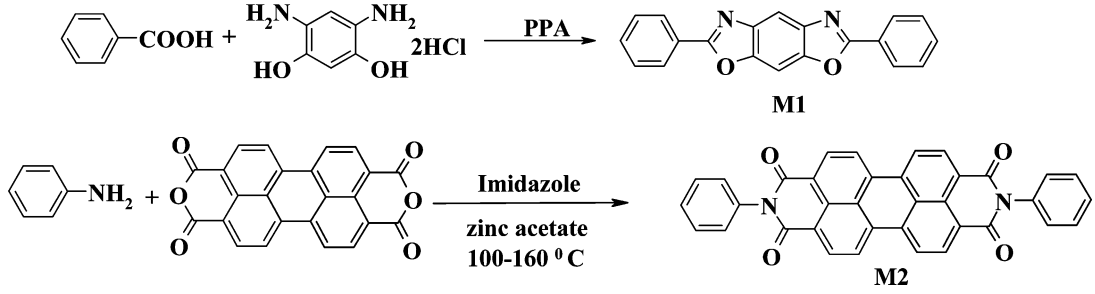

ment performed on a large number of devices (~20−25 devices of each polymer).

Results and Discussion

Synthesis, Characterization, and Polymerization. The synthesis of the copoly(benzoxazole) imides is given in Scheme 1 and the detailed procedure is given in the Supporting Information. A suitable diamine monomer (2,6-bis(*p*-aminophenyl)benzo[1,2-*d*;5,4-*d*′]bisoxazole) (bisoxazole diamine) containing the preformed benzobisoxazole unit was synthesized in PPA at 170 °C using 4-aminobenzoic acid and DADHB, following the literature procedure.[34] The diaminobisoxazole monomer was condensed with perylene-3,4,9,10-tetracarboxylic dianhydride (PTCDA) or 1,4,5,8-naphthalenetetracarboxylic dianhydride (NTCDA) to form the polyimides PerPBO or NapPBO in a one-step imidization in *m*-cresol and isoquinoline at 180−210 °C in good yields. A random copolymer of bisoxazole with perylene and naphthalene dianhydride NapPerPBO was also synthesized by taking 0.5 mol each of both dianhydrides and reacting with 1 equiv of bisoxazole diamine. Poly(*p*-phenylenebenzobisoxazole) (PBO) homopolymer was also synthesized by condensation polymerization using 2,4-diamino-1,5-benzenediol dihydrochloride (DADHB) and terephthalic acid in polyphosphoric acid (PPA) containing 83% P_2O_5 as reported in the literature.[1,3,35] There was a recent report where a carboxyl-terminated perylene bisimide was condensed with DADHB in PPA as a comonomer along with terephthalic acid as the main monomer.[36] This route could introduce only <2 mol % of perylene bisimide into the polymer backbone and only in a random manner. The imidization route adopted in our procedure has the advantage of producing exactly 1:1 alternating copolymer of perylene or napthhalene bisimide with benzobisoxazole units.

Model compounds which were representative of the benzobisoxazole unit (M1), and perylene bisimide unit (M2) were synthesized as shown in Scheme 2. The structure of monomer and copolyimides was confirmed by ^{1}H NMR recorded in deuterated sulfuric acid (D_2SO_4), solid-state ^{13}C NMR, and FT-IR spectroscopy. The ^{1}H NMR spectra of the model compounds (given in Supporting Information Figure S1) were used to structurally identify the peaks in the proton NMR spectra of the polymers. Figure 1 shows the labeled ^{1}H NMR spectra of polymers (a) NapPBO, (b) PerPBO, and (c) NapPerPBO. It could be seen from Figure 1c that the intensity of the four protons of the naphthalene ring (e′) was more than that due to the eight protons corresponding to that of perylene (e), indicating

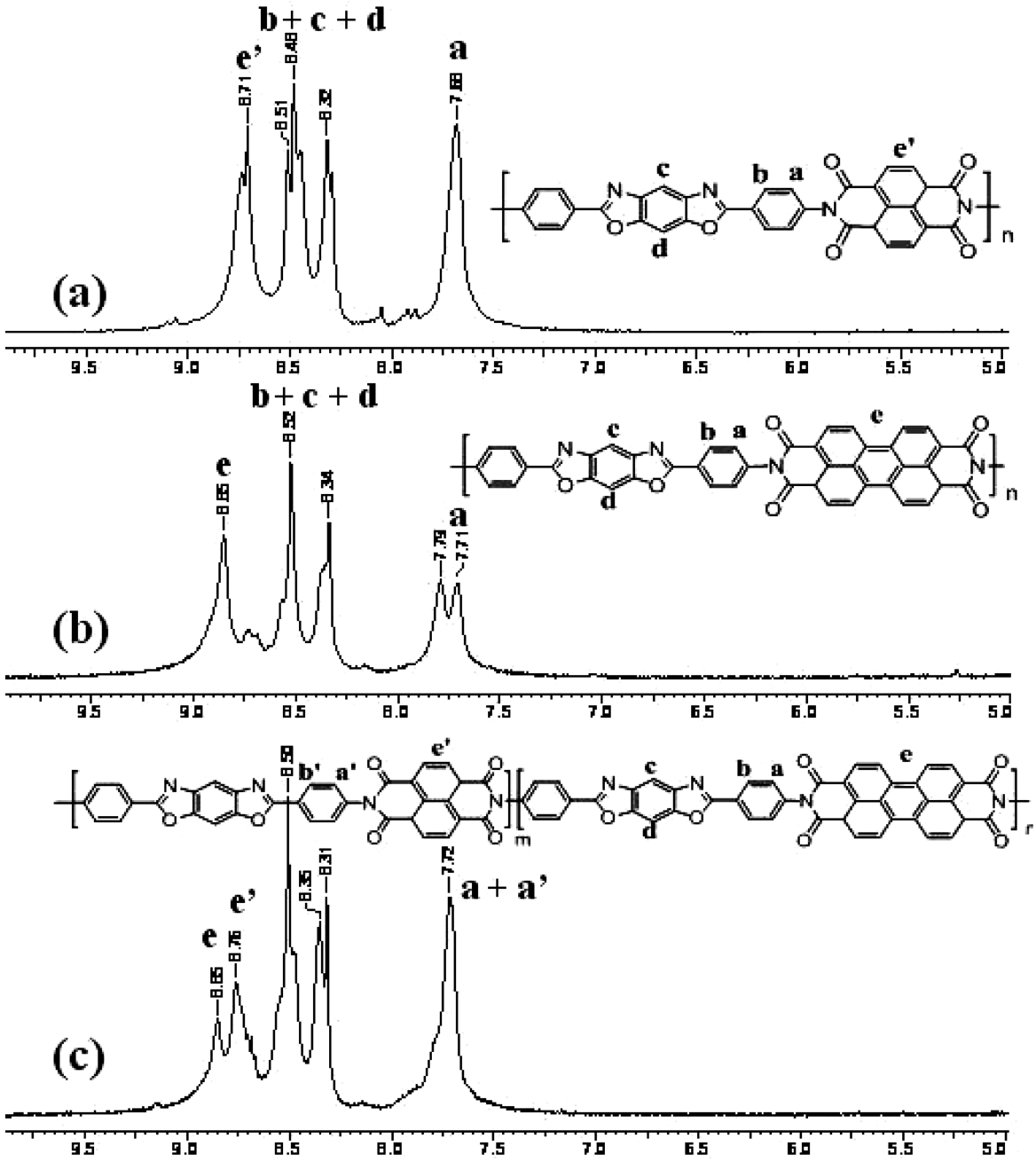

Figure 1. ^{1}H NMR spectra of (a) NapPBO, (b) PerPBO, and (c) NapPerPBO recorded in D_2SO_4.

higher incorporation of naphthalene compared to perylene into the random chain even though they were taken in equal mole ratio in the feed. An exact calculation of the incorporation of perylene with respect to naphthalene could not be made since there was a slight overlap of the perylene protons with those of the naphthalene protons; however, approximately it was calculated to be 70:30 naphthalene bisimide:perylenebisimide. Similarly, the solid-state ^{13}C NMR spectra of the naphthalene and perylene PBO copolymers (given in Supporting Information Figure S2) also clearly confirmed the structure of the polymers. The peak corresponding to carbonyl region of perylene and naphthalene appeared at 164 and 161 ppm, respectively. The peak corresponding to the C−O of benzoxazole ring appeared at 161 ppm.[37] In the PerPBO copolymer, these two were clearly differentiable at 164 and 161 ppm whereas in the NapPBO polymer the carbonyl as well as C−O of oxazole ring appeared as a single peak at 161 ppm. Completion of imidization in polymers could also be confirmed by FT-IR as shown in the Supporting Information Figure S3 by following the disappearance of the six-membered anhydride peak at 1774 cm^{-1} and the appearance of the characteristic imide peak at 1699 cm^{-1} and 1668 cm^{-1} (indicated by arrows) in the copolymers containing perylene.[27] In the naphthalene copolymer, the peak was observed at 1712 cm^{-1} and 1673 cm^{-1}. In the random copolyimide containing both perylene and naphthalene bisimide units in the backbone, two imide stretching peaks were observed at 1712 and 1702 cm^{-1} corresponding to naphthalene and perylene imides, respectively. In all the copolyimides, along with the imide stretching peak an additional peak was observed at 1610 cm^{-1} corresponding to the characteristic peak of benzoxazole ring. Thus, the NMR as well as FTIR spectra could successfully be utilized to confirm the incorporation of the various units in the copolymer backbone.

The insolubility of the copolymers in common organic solvents such as tetrahydrofuran (THF) and chloroform ($CHCl_3$) made molecular weight determination by size exclusion chro-

TABLE 1: Ten Percent Weight Loss Temperature (°C), Inherent Viscosity, and Yield of Homo- and Copolymers

polymer	10% wt. loss (°C)[a]	viscosity η_{inh} (dL/g)[b]	yield (%)[c]
PBO	666	5.27	96
PerPBO	535	0.24	80
NapPBO	432	0.15	86
NapPerPBO	496	0.23	80

[a] Temperature represents 10% weight loss in TGA measurements at heating rate of 10 °C/min under nitrogen. [b] Inherent viscosity measured in methanesulfonic acid (0.5 g/dL) at 30 ± 0.1 °C. [c] Final yield of the precipitated and washed sample.

matography (SEC) impossible. However, as is the practice in the case of similar rigid rod polymers reported in literature, the inherent viscosities were measured for the homo- and copolymers in methanesulfonic acid (MSA) at 30 °C.[1] The inherent viscosity values η_{inh} in dL/g are given in the Table 1. The homopolymer PBO which was polymerized in PPA had very high viscosities (5.27), and the polymer also was precipitated in the form of long fibers. However, the incorporation of the imides drastically reduced the viscosity of the copolymers, resulting in polymers with low inherent viscosities and average molecular weights.[38] The inherent visocisty values for PerPBO and random copolymer NapPerPBO was ~0.24 dL/g only. The NapPBO copolymer had the lowest viscosity among the copolymers. The direct comparison of the viscosity values of the homopolymer PBO with these poly(oxazoleimide)s is not justified since the conditions of polymerization were different. PBO is known to polymerize in high molecular weights from PPA as solvent. The polyimides of perylene and naphthalene bisimides reported in the literature are however not very high because of the inherent low solubility of the formed polymer.[39] Therefore, the inherent viscosity of 0.2 dL/g reported here indicated reasonably high molecular weight and the perylene containing polymers were obtained as dark red powders.

Supporting Information Figure S4 shows the TGA thermograms of the homo- and copolymers, and the 10% weight loss temperatures are given in Table 1. PBO had a 10% weight loss temperature above 660 °C, but with incorporation of the imide units, this was decreased to 535 °C for perylene and to 470 °C for naphthalene copolymer, respectively, indicating that the disruption of the rigid rod structure of PBO decreased the overall thermal stability of the system.

Liquid Crystalline Phases. Perylene or naphthalene bisimides are known to induce thermotropic liquid crystallinity in small molecules or oligomers whereas rigid rod polymers such as PBO are known to form lyotropic liquid crystalline phases in solvents such as MSA, PPA, etc., at a critical concentration from which polymer fibers having good mechanical properties can be spun. The three copolymers however did not exhibit any thermotropic liquid crystalline characteristics in the DSC thermogram or under the polarized light microscope (PLM). The formation of lyotropic mesophases (critical concentration) was studied by preparing different concentrations of polymer solutions in methanesulfonic acid (MSA). The sample dope was sealed between glass slides, annealed at 80 °C for 15 min, allowed to stand in a desiccator for 6 h, and then examined under the PLM.[40] It was found that PBO formed mesophases as confirmed by the observation of birefringence under crossed polarizers beyond a critical concentration of 5 wt % (clearing temperature 85 °C). A typical birefringent pattern as reported in the literature was observed.[40,41] For the PerPBO copolymer, the critical concentration was observed at ~6 wt % (clearing temperature 80 °C) and beautiful bright red birefringence typical

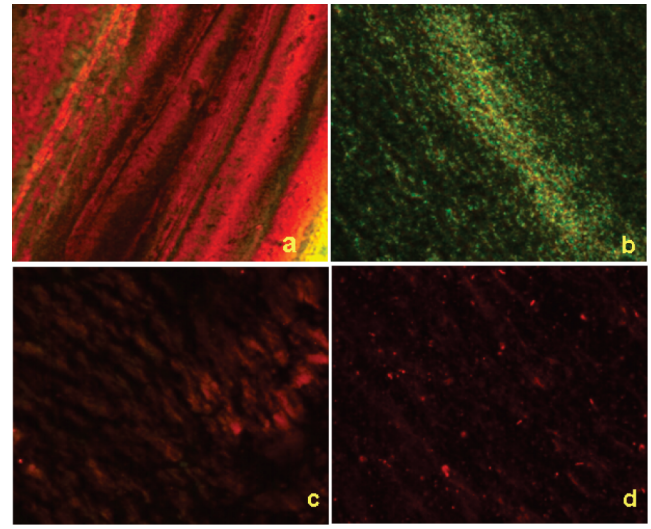

Figure 2. Crossed-polarized optical micrographs of (a) 5% PBO, (b) 10% NapPBO, (c) 6% PerPBO, and (d) 8% NapPerPBO in MSA.

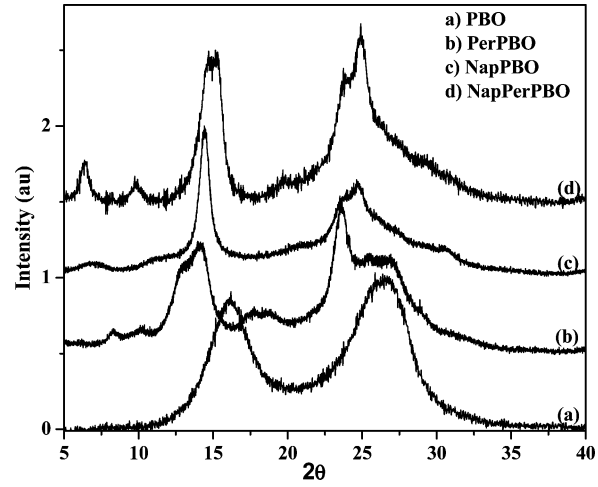

Figure 3. Wide-angle X-ray diffraction curves for homo- and copolymers.

of perylene was observed. The NapPBO copolymer's critical concentration was observed at 10 wt % (clearing temperature 80 °C) and green birefringence was observed. The NapPerPBO random copolymer showed red birefringence beyond a critical concentration of 8 wt % (clearing temperature 80 °C). Figure 2 shows the PLM images of the lyotropic phases of the polymers observed under crossed polarizers. The disruption of PBO packing by either perylene or naphthalene bisimide units did not destroy the mesophase tendency of the polymers.

In these imide-oxazole copolymers the bisimide units at every alternative position introduced a kink in the polymer backbone; however, this deviation from backbone linearity did not deleteriously affect the propensity for liquid crystal formation. Perylene and naphthalene bisimides are well-known for their $\pi-\pi$ stacking interaction in solutions as well as in solid state, and this also aids in parallel chain packing leading to the observation of mesophases.

WAXRD. The ordered structure of the copolymers was investigated by wide-angle X-ray diffraction (WAXRD) as shown in Figure 3, and all the related information is listed in Table 2. PBO has a characteristic WXRD pattern with two major diffraction peaks around $2\theta = 16.1°$ (~5.50 Å) and $2\theta = 26.5°$ (3.35 Å). The former corresponds to "side-to-side" distance on (200) plane (due to lateral packing of stacks: interstack) and

TABLE 2: XRD Results for the Copolymers

	2θ, deg		d spacing (Å)	
polymer	A	B	A	B
PBO	16.13	26.53	5.50	3.35
PerPBO	14.35	23.70	6.24	3.76
NapPBO	14.50	24.73	6.14	3.59
NapPerPBOs	14.06	23.75	6.02	3.76
	15.20	24.09	5.81	3.57

TABLE 3: Photophysical Properties of the Copolymer and Model Compounds in Methanesufonic Acid

polymer	absorption peak λ (nm)	emission λ_{max} (nm)	quantum yield $\phi_{bisoxazole}$[d]	quantum yield ϕ_{Per}[e]
M1	345, 365	391[a]	0.71	–
M2	510, 545, 580	615[c]	–	0.65
PBO	403, 428	438[b]	0.25	–
PerPBO	346, 475, 510, 547	390[a], 620[a,c]	0.008	0.51
NapPBO	349, 368, 386	390[a], 445[a]	0.013	–
NapPerPBO	349, 366, 386, 475, 510, 545	390[a], 445,[a] 618,[a,c]	0.020	0.59

[a] Excitation at 345 nm. [b] Excitation at 403 nm. [c] Excitation at 545 nm. [d] The fluorescence quantum yields were obtained upon excitation at 343 nm and were measured using anthracene as a standard; for PBO the excitation wavelength was 402 nm and quinine sulfate was the reference. [e] The fluorescence quantum yields were obtained upon excitation at 510 nm and were measured using rhodamine-6G as a standard.

the latter to the "face-to-face" distance on (010) plane (stacking: intrastack) between two neighboring rod molecular chains of poly(benzobisoxazole)s, respectively.[42] The copolymers PerPBO and NapPBO as well as NapPerPBO had several peaks in the $2\theta = 3-35°$ range. In all copolymers the periodic order corresponding to the 5.50 Å side-to-side spacing was shifted to higher *d* spacing. The introduction of perylene or naphthalene bisimide units is expected to increase the side-to-side distance in the copolymers. The 3.36 Å which corresponded to the face-to-face PBO stacking was observable, though only as a shoulder in the case of the NapPerPBO and NapPBO polymer. The PerPBO polymer had a sharp peak ~3.7 Å, indicating better ordering. This corresponded to the $\pi-\pi$ stacking in the perylene aromatic ring. Normally the perylene $\pi-\pi$ stacking is observed at ~3.5 Å.[43] The expansion in this $\pi-\pi$ stacking is due to the incorporation of benzoxazole units between the perylene units. This $\pi-\pi$ stacking peak in the NapPBO polymer was observed at 3.59 Å. In the NapPerPBO random copolymer, sharp peaks were observed at both 3.57 and 3.76 Å corresponding to the $\pi-\pi$ stacking of both perylene and naphthalene. Thus, the WAXRD also gave structural proof for the incorporation of the bisimides into bisoxazole backbone.

Photophysical Studies. ***Absorption Spectra.*** The absorption and emission spectral data of the copolymers and the model compounds recorded in MSA are summarized in Table 3. Figure 4 shows the UV−vis absorption spectra of the polymers and model compounds recorded in MSA. PBO exhibited characteristic absorption peaks at 403 and 428 nm.[42] In the PerPBO copolymer the broad peak at ~346 nm is attributed to bisoxazole unit, and the latter three peaks at 475, 510, and 547 nm are the characteristic absorptions of perylene bisimide. In the NapPBO copolymer, the absorption of naphthalene bisimide was overlaid by that of the bisoxazole absorption, and a broad peak at 368 nm having a shoulder at 386 nm was observed. In the NapPerPBO random copolymer of perylene and naphthalene bisimide with bisoxazole also the peaks lower than 400 nm corresponded to the absorption of naphthalene bisimide and bisoxazole whereas the three peaks beyond 450 nm corresponded to that of perylene bisimide.

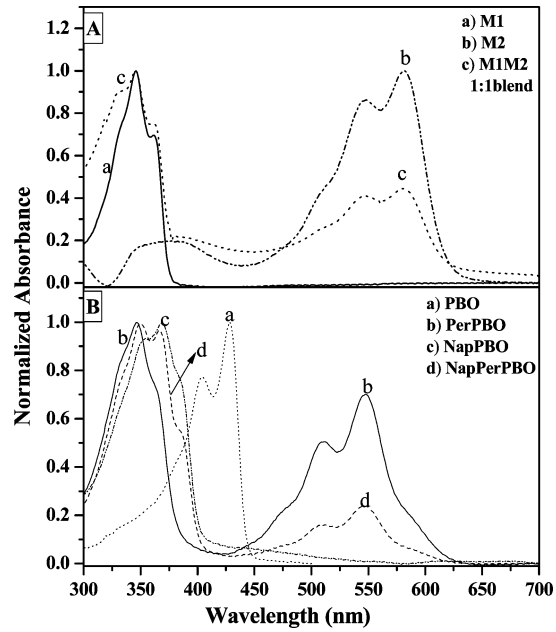

Figure 4. UV−vis absorption spectra of (A) model compounds M1, M2, and a 1:1 blend of M1 and M2, and (B) the copolymers along with PBO recorded in methanesulfonic acid (MSA).

Figure 4A shows the stackplot of the absorption spectra of the model compounds M1 and M2 along with that of the 1:1 molar blend of M1 and M2 recorded in MSA. The absorption corresponding to the perylene unit was blue-shifted in the copolymers compared to the perylene bisimide model compound M2. The coefficient of absorption of the bisoxazole is much higher compared to that of perylenebisimide; therefore, the 1:1 molar blend of M1 and M2 had lower intensities of absorption for perylene. The absorption of the blend resembled a linear superposition of the respective model compounds. This difference in behavior of the copolymers compared to the blend is a clear indication that in the copolymers there was a perturbation of the electronic transition in the ground state upon covalent linkage. Comparing the absorption spectra of the PerPBO copolymer with the random copolymer NapPerPBO, the peak intensities of the perylene part was much reduced in the latter. This is due to lower incorporation of perylene as well as due to the naphthalene diimide absorption also enhancing the optical density at 350 nm in the latter. The absorption of PBO was red-shifted by ~70 nm compared to its own model compound M1 due to the planarity and rigidity of the benzobisoxazoles which result in increased conjugation upon polymerization. On the other hand, the absorption of the benzoxaole moiety in all the copolymers with perylene or naphthalene bisimide was blue-shifted by 80 nm compared to the homopolymer PBO. The imide linkage at every alternate position in the copolymers resulted in a disruption of the extended π network of the PBO promoting strong hypsochromic shift.

The emission spectra were recorded and the quantum yields determined (Table 3) for the model compounds and copolymers in MSA by exciting at both the bisoxazole absorption λ_{max} of 345 nm as well as at the perylene absorption λ_{max} of 545 nm. Figure 5 shows the absorption (dotted line) and emission (straight line) spectra of the model compounds M1 and M2 showing the spectral overlap of the bisoxazole emission with that of the perylene absorption. This is the primary requirement for Förster energy transfer between donor (D)−acceptor (A) systems.[44] Although heterocyclic benzobisoxazoles are electron deficient, compared to the highly electron-withdrawing perylene

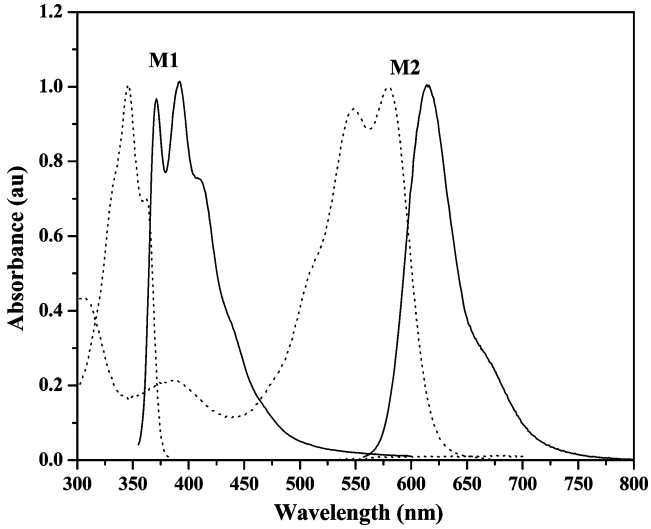

Figure 5. Absorption (dotted line) and emission (straight line) spectra of model compounds M1 and M2 in methanesulfonic acid (MSA) (0.1 OD solutions).

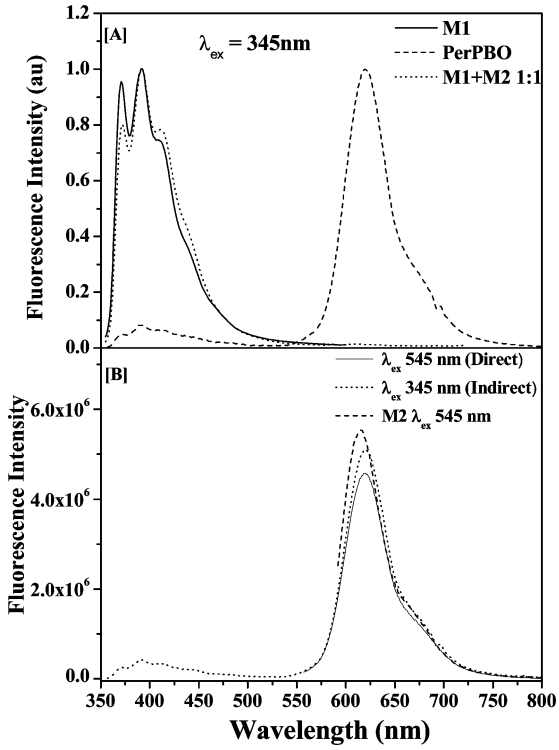

Figure 6. Emission spectra of M1 and a 1:1 molar mixture of M1 and M2 along with PerPBO in methanesulfonic acid (MSA) (0.1 OD solutions); excitation: 345 nm.

bisimides, the bisoxazole has very weak electron-accepting properties; hence, it can act as a donor to perylenebisimides.[45] Since there was no overlap between the absorption spectra of the bisoxazole and perylene units, it was possible to selectively excite either of them by choosing the appropriate excitation wavelength. An effective method to study the energy/electron transfer resulting from photoexcitation between a covalently linked D−A molecule is to examine the photoluminescence quenching observed upon blending the individual components.[44] Figure 6A top shows the emission spectra of the copolymer PerPBO along with that of M1 and a 1:1 blend of M1 and M2 upon excitation at 345 nm (all solutions having 0.1 OD at the bisoxazole absorption maxima of 347 nm). The 1:1 blend and

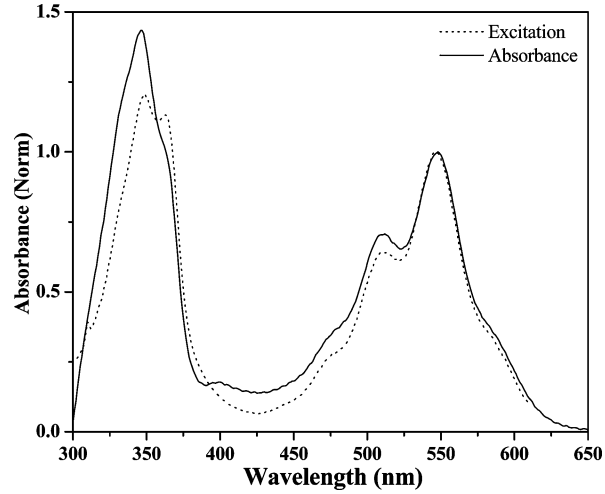

Figure 7. Normalized absorption (solid lines) and excitation (dotted lines) spectra of the PerPBO copolymer in methanesulfonic acid (MSA).

M1 exhibited almost identical emission at λ_{max} of 390 nm. M2 did not have any appreciable emission upon excitation at 345 nm (not shown in figure). The PerPBO copolymer, on the other hand, had almost complete quenching (~92%, $\phi_{MSA} = 0.008$) of the bisoxazole emission at 390 nm but had an intense peak corresponding to perylene emission at λ_{max} of 620 nm, indicating a near complete energy transfer. The excitation spectra were recorded to examine if energy transfer took place from oxazole to perylene unit. Figure 7 compares the absorption and excitation spectra for PerPBO copolymer measured by monitoring the emission of the acceptor perylene bisimide at 620 nm. Besides the absorption of perylene, an absorption band corresponding to oxazole unit with maxima at 347 nm was also present in the excitation spectra. This suggested that upon photoexcitation, energy transfer channels existed between the bisoxazole to perylene units. However, the intensity of the sensitized or indirect emission from perylene was not 100%. It was slightly quenched (7%) when compared to the reference compound. This slight quenching of the emission indicated that apart from energy transfer, an additional process of quenching such as electron transfer from bisoxazole to perylene was also involved. The excitation spectra in Figure 7 also showed that a clear difference existed between the absorption and excitation spectra in the bisoxazole absorption region of 300−400 nm. This indicated that direct electron transfer also occurred upon excitation of the oxazole moiety.[46]

Figure 6B bottom compares the emission from M2 and copolymer PerPBO both upon direct (perylene) excitation at 545 nm and sensitized/indirect excitation at 345 nm. The indirect emission from PerPBO was higher in intensity compared to the emission upon direct excitation of the perylene bisimide unit. This observation is very similar to that reported by J. Pan et al. where dendrons with a perylene core and oxadiazole periphery exhibited strong light harvesting potential and gave intense perylene emission upon excitation of the oxazole periphery compared to direct perylene excitation.[29] Similarly in the copolymer PerPBO, the PBO units act as a funnel channeling energy to the perylene units. If there were no other quenching pathway, the emission intensity from perylene bisimide upon direct excitation (545 nm) should have been same as that of M2. However, the perylene emission from the copolymer upon direct excitation also was quenched (~18%) and quantum yields of the perylene emission were also lower ($\phi_{MSA} = 0.51$) compared to that from M2 ($\phi_{MSA} = 0.65$). Photoexcitation of the perylene unit cannot result in energy transfer, but charge

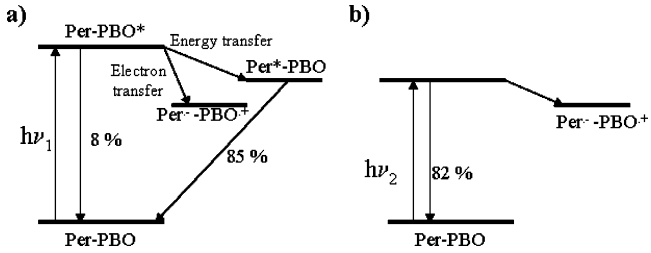

Figure 8. Schematic diagram of the PerPBO copolymer showing energy and electron transfer pathways upon excitation of (a) PBO λ_{ex}: 345 nm and (b) perylene λ_{ex}: 545 nm.

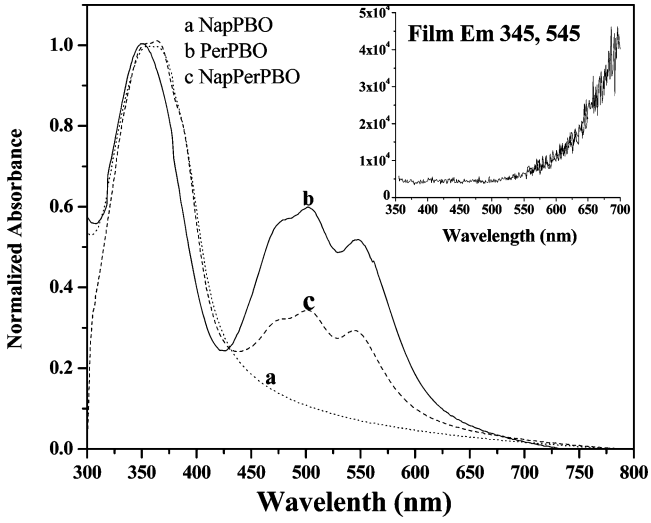

Figure 9. Normalized absorption spectra of the copolymers in solid state (film).

separation can still occur, resulting in quenching of the perylene fluorescence. Figure 8 shows the schematic representation of the possible energy and electron transfer pathways upon excitation at 345 or 545 nm.

An important point of consideration in this energy/electron transfer processes is the fact that the PBO units are protonated in MSA, which could result in enhanced delocalization and planarization of the heterocyclic and aromatic ring, leading to better electronic coupling.[47,48] This would facilitate the energy/electron transfer from bisoxazole to perylene upon exitation at 345 nm corresponding to the λ_{max} absorption of bisoxazole.

Supporting Information Figure S5 shows the emission from the copolymers NapPBO and NapPerPBO upon excitation at 345 nm. The polymer showed characteristic naphthalene emission at λ_{max} of 445 nm. The NapPerPBO random copolymer showed emission from both naphthalene as well as from perylene units. The indirect excitation resulted in higher intensity of perylene emission compared to direct excitation as was observed in the case of PerPBO copolymer. The additional gradient in the energy levels from the PBO unit to the perylene units due to the presence of naphthalene units should benefit the energy transfer process.

Photoexcitation studies were carried out in the solid state for the various copolymers. Films were prepared by spin-coating from MSA solution, washing in deionized water, and leaving it in deionized water for several hours followed by washing with acetone and drying in a vacuum oven at 60 °C overnight. Figure 9 shows the absorption (inset: PL for PerPBO copolymer) spectra of the film samples. The absorption showed a change in the peak intensity ratios of the 0−0, 0−1 transitions along with a red shift of the onset in perylene which is a signature of H-type or face-to-face $\pi-\pi$ stacking interaction of the perylene aromatic cores.[49] The PBO homopolymer film showed a weak red-shifted emission at 498 nm (which has been attributed to excimer or aggregate formation),[50] but the emission was totally quenched in the copolymer films for both direct and indirect excitation.[27] The complete quenching of fluorescence of both chromophores demonstrated efficient chain packing taking place in the solid state.

Electrochemical Properties. The effect of molecular structure upon electrochemical properties was explored through the measurement of the electrochemical reduction using cyclic voltammetry (CV). The polymers were deposited as thin films from MSA onto the platinum working electrode which was immersed in deionized water overnight, washed with acetone, and dried in vacuum oven at 60 °C, and then their cyclic voltammograms were recorded in 0.1 M $TBAPF_6$/acetonitrile solution. The CV measurement was repeated to check reproducibility, and this process of film deposition was found to be perfectly reproducible for CV measurement. Table 4 gives the redox potentials and the HOMO/LUMO values calculated for the model compounds and the copolymers along with that of the homopolymer PBO. The potential was measured against Ag/Ag^+ reference electrode (Ag wire in 0.01 M $AgNO_3$) using the internal standard ferrocene/ferrocenium (FC/FC^+) redox system. Perylenebisimides generally exhibit two reversible reduction peaks in the cathodic scan corresponding to the first and second one-electron stepwise reduction of the perylene core to the monoanion and dianion, respectively.[51] M2 was easily reduced, exhibiting two quasireversible reduction peaks at −1.37 and −1.04 V, respectively, at a scan rate of 0.2 V/s. The cyclic voltammogram of model compound M1 could not be recorded in solution (acetonitrile) due to poor solubility, neither could it be drop-casted as a thin film. Therefore, for comparison the cyclic voltammogram was recorded for the diamine monomer (bisoxazole diamine) which was soluble in DMF. The reduction potential of benzoxazole is known to be very high (−2.3 V), and DMF as a solvent is known to be stable up to −3 V. Bisoxazole diamine exhibited two reversible peaks at −2.3 and −2.7 V. The cyclic voltammogram of the polymers coated as thin film on a platinum working electrode in 0.1 M $TBAPF_6$/acetonitrile solution is given in the Supporting Information Figure S6. The homopolymer PBO exhibited a reduction peak at −2.36 V which is well matched with that reported in the literature.[52] PerPBO copolymer showed a single reversible reduction peak at −1.34 V due to reduction of perylene moiety, and upon increasing the potential further, another reduction peak was observed at −2.48 V corresponding to reduction of the bisoxazole group. One irreversible oxidation peak of bisoxazole also appeared during the anodic scan at 1.5 eV. NapPBO and NapPerPBO polymers also exhibited reduction peaks at −1.36 and −1.37 V, respectively, and a second reduction peak for bisoxazole at same reduction potential as that observed in the case of PerPBO copolymer. It is thus evident from the CV data that the reduction potential for perylene- or napththlene-containing copolymers was low compared to that of poly(benzobisoxazole). Unlike the model compound M2, the PBO copolymers with perylene or naphthalene bisimide had only a single reduction peak corresponding to that of the imide. It has been reported in literature that in the homologue diimides, perylene, terrylene, and quaterrylene, as the conjugation increased, the spacing between the two successive 1e reduction waves decreased until the two peaks completely overlapped.[51] Similarly, in the PBO copolymers also the two reduction peaks merged into one single 2e peak, due to the extensive π overlap

TABLE 4: Redox Potential and HOMO/LUMO Values of Model Compounds and Copolymers

polymer/model compound	E_{pc1}/E_{pa1}(V)	E_{pc2}/E_{pa2}(V)	nonperylene (bisoxazole) part in polymers E_{pc}/E_{pa} (V)	LUMO (eV)	HOMO (eV)	E_g(opt) (eV)
bisoxazole diamine	−2.30/−2.28	−2.70/−2.60	−	−2.50	−5.60	3.10
M2	−1.04/−0.84	−1.37/−1.07	−	−3.80	−5.86	2.06
PBO	−2.36/−1.97	−	−	−2.83	−5.60	2.77
PerPBO	−	−1.34/−1.08	−2.48/−2.35	−3.70	−5.76	2.06
NapPBO	−	−1.36/−1.20	−2.47/−2.35	−3.68	−6.56	2.88
NapPerPBO	−	−1.37/−1.18	−2.47/−2.35	−3.68	−5.74	2.06

[a] E_{pc} = cathodic peak potential; E_{pa} = anodic peak potential. [b] Each measurement is calibrated with the ferrocene/ferrocenium redox system vs Ag/Ag^+.

among the perylene and naphthalene bisimide units existing in the polymer. The cyclic voltammograms of the copolymers indicated that there was no marked difference of reduction potentials between perylene and naphthalene units in the polymer backbone since their LUMO values were nearly same.[53] The LUMO energy levels of the polymer and model compounds were estimated based on the onset of the polymer reduction peak and reference energy level of ferrocene (4.8 V below the vacuum level) according to $E_{LUMO}(eV) = -e \times (E^{red\ onset} + 4.8)$ below the vacuum level.[22] The HOMO energy levels were estimated from the optical band gap and the LUMO energy level and are listed in Table 4. The HOMO/LUMO energy level values for free model compound (M2) and in copolymers were nearly the same for perylene as well as for the bisoxazole group, as their reduction potential remained the same upon polymerization. In case of the PerPBO and NapPerPBO copolymers, the HOMO energy level values were −5.76 and −5.74 eV, respectively, and in case of NapPBO, the corresponding HOMO energy value was −6.56 eV. On other hand, the HOMO energy value for the benzobisoxazole part was −5.60 V[52] which was above the HOMO of perylene and naphthalene. The LUMO energy level value for the benzoxazole part was much higher (−2.5 eV) than either the perylene or naphthalene group. Thus, these energy level values gave additional support to energy and electron transfer from bisoxazole to perylene upon excitation of the bisoxazole.[44]

Device Characteristics. The devices fabricated from these polymers showed excellent saturation n-type transport with Al as the source/drain and gate electrode as indicated from the gate-dependent output curve and transconductance curves shown in Figure 10 for PerPBO and NapPerPBO. The saturation region carrier mobility was calculated with the standard transconductance characteristics of the drain source current (I_{ds}) in the saturation mode: $I_{ds} = (\mu_{FET}WC_0/2L)(V_g - V_t)^2$ where μ_{FET} is the field effect electron mobility, C_0 is the effective capacitance, W the channel width, L the channel length of the transistor, V_g and V_t are the gate and threshold voltages, respectively, and the results are summarized in Table 5. All the FETs based on these polymer systems exhibited good current modulation with an on/off ratio greater than 10^2 upon annealing (150−160 °C for 30 min). In contrast, the unannealed samples displayed poor mobilities. The large improvement upon annealing is illustrated by the values of μ_{FET} for PerPBO before and after annealing (Table 5).[30,54] Supporting Information Figure S7 shows the SEM images of PerPBO copolymer before and after annealing at 160 °C for 1 h, clearly showing differences in morphology upon annealing. Annealing can provide the polymer chains enough energy to access better conformational arrangement and sufficient time to have optimized alignment of the polymer chain within the microdomain itself and in the process decreasing the trap-state density. Specifically, annealing can introduce better phase separation in the segmented copolymer, which can explain

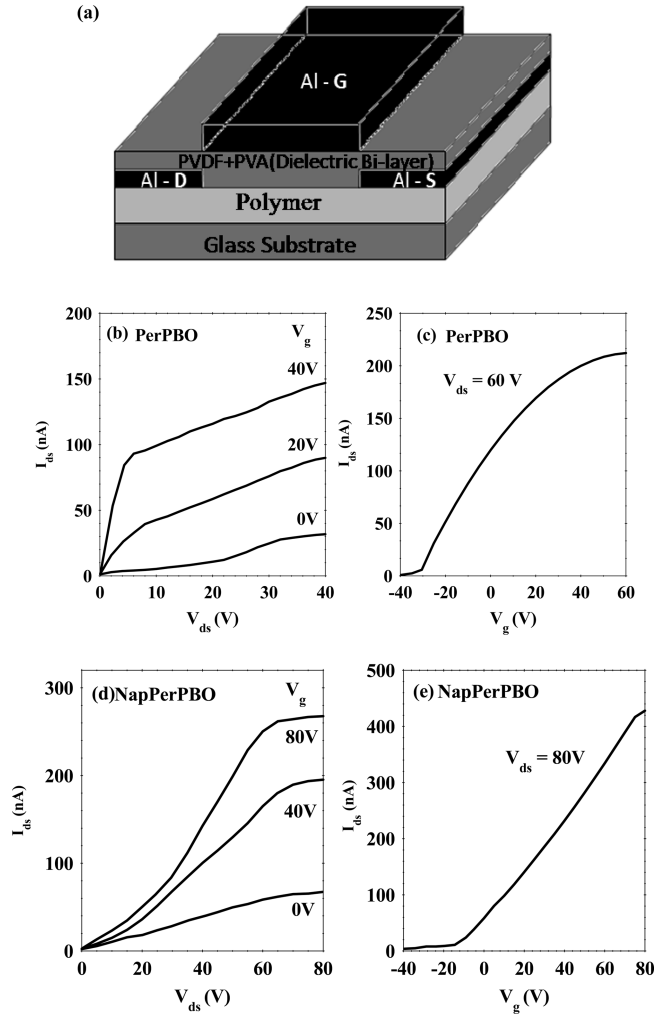

Figure 10. (a) Schematic of a bottom gate OFET. (b, c) Transistor curves for PerPBO polymer. (d, e) Transistor curves for NapPerPBO polymer.

TABLE 5: OFET Characteristics of the Copolymers

polymer	μ_e ($cm^2\ V^{-1}\ s^{-1}$)	I_{on}/I_{off}
PBO	$(1 \pm 0.16) \times 10^{-4}$	6×10^2
PerPBO	$(0.8 \pm 0.18) \times 10^{-4}$ $(6.2 \times 10^{-6})^a$	2×10^3
NapPBO	$(8 \pm 1.04) \times 10^{-4}$	2×10^3
NapPerPBO	$(2 \pm 0.31) \times 10^{-3}$	4×10^2

[a] Without annealing.

the higher transport properties.[30] The observation from a large number of devices tested showed a trend where the random copolymer containing both perylene and naphthalene bisimides exhibited the highest mobility of 0.2×10^{-2} $cm^2/(V\ s)$ with an on/off ratio of 4×10^2. The alternating copolymer of perylene

bisimide with benzobisoxazole, i.e., PerPBO, had mobilities similar to that of the homopolymer PBO. The copolymer naphthalene bisimide with benzobisoxazole (NapPBO) ($I_{ds}-V_{ds}$ characteristics and the transconductance curves are given in Supporting Information Figure S8) showed charge carrier mobility which was 1 order of magnitude higher than that of the perylene-based copolymer and follows the trend where μ_{FET} for naphthalene derivatives show greater values than μ_{FET} of perylene derivatives.[55]

The transport in the random copolymer can be described in terms of a 1-D Anderson localization model. Introduction of impurities or defects (which are like energetic barriers) cause the scattering of the electron wave function thus affecting the wave propagation.[56] If the barrier is not large enough, then the electron continues in its extended state. But in the case of multidimensional (for example in quasi-one-dimensional-variable range hopping) transport, the charge carrier primarily may hop along a "one-dimensional" chain, but it can also occasionally have an intrachain hop to avoid energetic disorder, and thus the wave function can still remain delocalized. So under the assumption of one-dimensional charge transport when a segment of a guest polymer is introduced in the host matrix of the polymer, the transport properties of this random copolymer (host + guest) thus formed are less compared to those of the corresponding parent homopolymers because of the additional scattering in the electronic wave propagation. The absence of a decrease of μ_{FET} in the present case of the random copolymer indicates the equivalence of the naphthalene transport levels with respect to the perylene transport levels as also suggested by the similar LUMO levels. Additionally, the higher μ_{FET} of the random copolymer can be attributed to better lateral structural ordering as indicated from the relatively high intensity and sharp peaks corresponding to $\pi-\pi$ stacking of the random copolymer in WXRD and the improved persistence length compared to NapPBO. This structural ordering can arise from an improved stacking of the NapPBO in the confined and comparatively more rigid structure of PerPBO, thus improving the transport properties of the random copolymer. The comparatively high μ of the random copolymers can also be explained in terms of a Semiclassical Marcus model. The larger μ in the NaphPer-PBO copolymer can arise from the better structural ordering, which is the outcome of a better stacking of the naphthalene units in the confined and more rigid structure of Per-PBO which can decrease the reorganization energy. Additionally the $\pi-\pi$ stacking distance could be less in this system, resulting in a higher value of the transfer integral. The interplay of these parameters can result in a more favorable μ for the random copolymer than for the other polymers chosen.

Photocurrent (I_{ph}) measurements of the FET structures (Figure S9) also provide an insight into the carrier generation and transport mechanisms and ascertain the contribution of each of the homopolymers. The photocurrent spectra largely follow the combined absorption as indicated by the response at $\lambda = 532$ nm and $\lambda = 405$ nm for the different polymer systems. Upon photoexcitation with a source at the wavelength corresponding to the absorption with the V_g and V_{ds} held constant, I_{ds} exhibits an increase. The I_{ph} magnitude in the random copolymer NapPerPBO indicates a higher contribution from the NapPBO absorption compared to PerPBO absorption region. Nevertheless, a small but discernible I_{ph} was present at $\lambda = 532$ nm corresponding to the perylene absorption. It was observed that the current induced by $\lambda = 405$ nm excitation has a stronger electric field dependence (especially at higher field) compared to the current induced by $\lambda = 532$ nm excitation (Figure 11).

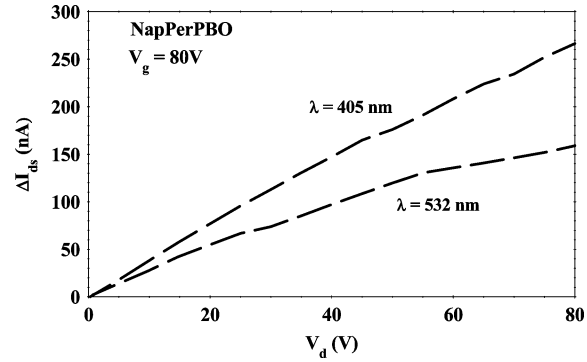

Figure 11. Change in I_{ds} in the NapPerPBO FET upon photoexcitation incident from the glass substrate side at different wavelengths (magnitude normalized for equivalent power/area).

This behavior can be attributed to the field-dependent carrier generation from the NapPBO unit or the field-dependent carrier transport mechanism.[57] The difference in the behavior of the $\Delta I_{ds}(V)$ arising from the two types of carriers points to the higher field-dependent carrier generation term in the NapPBO segments of the chain.

Conclusion

An alternating copolymer of benzobisoxazole and perylenebisimide and/or naphthalene bisimide was synthesized, and the effect of molecular structure upon electronic and redox properties were studied. The presence of the imide linkage at every alternate position did not deleteriously affect the mesophase formation ability of these copoly(benzoxazole imide)s. All the oxazole-imide copolymers exhibited lyotropic mesophases in MSA at critical solution concentrations similar to that of the homopolymer PBO. The PerPBO copolymer showed interesting funneling behavior upon indirect excitation at the bisoxazole wavelength. Almost exclusive emission from perylene units was observed at 620 nm upon selective excitation of bisoxazole (345 nm), indicating highly efficient (>90%) energy transfer from bisoxazole to perylene. The emission at 620 nm was higher in intensity upon indirect excitation (345 nm) compared to the direct excitation of the perylene moiety at 545 nm. The quenching of perylene fluorescence upon direct excitation showed that electron transfer also played an important role. There was complete quenching of fluorescence in spin-coated films upon both direct as well as indirect excitation. The copolymer solutions in MSA were protonated, resulting in improved planarity and leading to better electronic coupling and energy transfer from bisoxazole to perylene/naphthalene bisimide units. On the other hand, the geometry was different in the solid state, resulting in total quenching of florescence of both bisoxazole and perylene units. The electrical transport characteristics of these copolymers were determined in an FET device configuration which showed their n-type charge transport nature. The random copolymer exhibited higher mobility, on−off ratio, and wavelength-dependent I_{ds} photoresponse.

Acknowledgment. We thank the network project NWP0023, DMSRDE project GAP272826, and DST project GAP 277826 for financial support. The authors thank Mr. Mangesh Mahajan and Mr. Ketan Bhotkar, NCL-Pune, for XRD and SEM measurements, respectively.

Supporting Information Available: ^{1}H and solid-state ^{13}C NMR of monomer and polymer, FTIR spectra, TGA, fluorescence studies, cyclic voltammogram of polymers, SEM of

polymers before and after annealing, gate-dependent output curve and transconductance curves for PBO and NapPBO, and wavelength-dependent I_{ds} photoresponse curve for random copolymers. This material is available free of charge via the Internet at http://pubs.acs.org.

References and Notes

(1) Mehdi, A.; Doetze, J. S.; Katekyn, L.; Mary, B. *Polym. Rev.* **2008**, *48*, 230.
(2) Lysenko, Z. U.S. Patent 4,766,244, 1988.
(3) Ying, H. S. *Prog. Polym. Sci.* **2000**, *25*, 137.
(4) Kuroki, T.; Tanaka, Y.; Hokudoh, T.; Yabuki, K. *J. Appl. Polym. Sci.* **1997**, *65*, 1031.
(5) Han, G. C.; Kumar, S. *J. Appl. Polym. Sci.* **2006**, *100*, 791.
(6) Maksudal, M. A.; Jenekhe, S. A. *Chem. Mater.* **2002**, *14*, 4775.
(7) Amit, B.; Jenekhe, S. A. *J. Phys. Chem. B* **2002**, *106*, 6129.
(8) Eilaf, A.; Felix, S. K.; Hao, X.; Jenekhe, S. A. *Macromolecules* **2009**, *42*, 8615.
(9) Liou, G.-S. *Macromol. Chem. Phys.* **2000**, *201*, 1141.
(10) Che, X. Q.; Sun, Q.; Huang, Y.; Cai, W. *J. Appl. Polym. Sci.* **2008**, *110*, 1891.
(11) Preston, J.; Dewinter, W. F.; Black, W. B. *J. Polym. Sci., Part A: Polym. Chem.* **1969**, *7*, 283.
(12) Steve, L.-C.; Chang, K.-C.; Huang, Y.-P.; Tsai, S.-J. *J. Appl. Polym. Sci.* **2003**, *88*, 2388.
(13) Steve, L.-C.; Luo, G.-W.; Chen, H.-T.; Chuang, S.-W. *J. Polym. Sci., Part A: Polym. Chem.* **2005**, *43*, 6020.
(14) Liou, G.-S. *J. Polym. Sci., Part A: Polym. Chem.* **1999**, *37*, 4151.
(15) Sirringhaus, H.; Tessler, N.; Friend, R. H. *Synth. Met.* **1999**, *102*, 857.
(16) Iain, M.; Martin, H.; Clare, B.; Kristijonas, G.; Iain, M.; Maxim, S.; David, S.; Steve, T.; Robert, W.; Weimin, Z.; Michael, L. C.; Joseph, R.; Micheal, D.; Micheal, F. *Nat. Mater.* **2006**, *5*, 328.
(17) Wen, Y.; Liu, Y. *Adv. Mater.* **2010**, *22*, 1.
(18) Chen, Z.; Zheng, Y.; Yan, He.; Facchetti, A. *J. Am. Chem. Soc.* **2009**, *131*, 8.
(19) Gardon, L. T.; Power, J. M.; Jeskey, S. J.; Mathias, L. J. *Macromolecules* **1999**, *32*, 3598.
(20) Johnson, P. O.; Jenekhe, S. A. *Macromolecules* **1990**, *23*, 4419.
(21) Manoj, A. G.; Alagiriswamy, A. A.; Narayan, K. S. *J. Appl. Phys.* **2003**, *94*, 4088.
(22) Durban, M. M.; Kazarinoff, P. D.; Luscombe, C. K. *Macromolecules* **2010**, *43*, 6348.
(23) Schmidt, H.; Oh, J. H.; Sun, Y.-S.; Deppisch, M.; Krause, A.-M.; Radacki, K.; Holger, B.; Martin, K.; Peter, E.; Frank, W. *J. Am. Chem. Soc.* **2009**, *131*, 6215.
(24) Kevin, C. S.; Landis, C.; Sarjeant, A.; Katz, H. E. *Chem. Mater.* **2008**, *20*, 3609.
(25) Pawel, G.; Damien, B.; Aleksandra, K.; David, D.; Stephanie, P.; Verilhac, J.-M.; Malgorzata, Z.; Adam, P. *J. Mater. Chem.* **2010**, *20*, 1913.
(26) Chen, H. Z.; Ling, M. M.; Mo, X.; Shi, M. M.; Wang, M.; Bao, Z. *Chem. Mater.* **2007**, *19*, 816.
(27) John, A. M.; Minas, M. S.; Sharma, G. D.; Balaraju, P.; Roy, M. S. *J. Phys. Chem. C* **2009**, *113*, 7904.
(28) Wang, Z. Y.; Qi, Y.; Gao, J. P.; Sacripante, G. G.; Sundararajan, P. R.; Duff, J. D. *Macromolecules* **1998**, *31*, 2075.
(29) Pan, J.; Zhu, W.; Li, S.; Zeng, W.; Cao, Y.; Tian, H. *Polymer* **2005**, *46*, 7658.
(30) Sven, H.; Micheal, S.; Thelakkat, M. *Appl. Phys. Lett.* **2008**, *92*, 093302.
(31) Gupta, D.; Kabra, D.; Kolishetti, N.; Ramakrishnan, S.; Narayan, K. S. *Adv. Funct. Mater.* **2007**, *17*, 226.
(32) Tashiro, K.; Hama, H.; Yoshino, J.-I.; Abe, Y.; Kitagawa, T.; Yabuki, K. *J. Polym. Sci., Part B: Polym. Phys.* **2001**, *39*, 1296.
(33) Amit, B.; Jenekhe, S. A. *J. Am. Chem. Soc.* **2003**, *125*, 13656.
(34) Evstalev, V. P.; Braz, G. I.; Yakubovich, A. Y. *Chem. Heterocycl. Compd.* **1970**, *6*, 682.
(35) Wolf, J. F.; Arnold, F. E. *Macromolecules* **1981**, *14*, 909.
(36) Xu, X.-H.; Liu, X.-Y.; Zhuang, Q.-X.; Han, Z.-W. *J. Appl. Polym. Sci.* **2010**, *116*, 455.
(37) Joanne, H. P.; Preston, J.; Samulski, E. T. *Macromolecules* **1993**, *26*, 1793.
(38) Sean, M. M.; Wang, Z. Y. *J. Polym. Sci., Part A: Polym. Chem.* **2000**, *38*, 3467.
(39) Jancy, B.; Asha, S. K. *J. Polym. Sci., Part A: Polym. Chem.* **2009**, *47*, 1224.
(40) Yu, S. C.; Gong, X.; Chang, W. K. *Macromolecules* **1998**, *31*, 5639.
(41) Kumar, S.; Dand, T. D.; Arnold, F. E.; Bhattacharyya, A. R.; Min, B. G.; Smalley, R. E.; Ramesh, S.; Willis, P. *Macromolecules* **2002**, *35*, 9039.
(42) Gao, P.; Wang, S.; Wu, P.; Han, Z. *Polymer* **2004**, *45*, 1885.
(43) Shi, M.-M.; Chen, H.-Z.; Shi, Y.-W.; Sun, J.-Z.; Wang, M. *J. Phys. Chem. B* **2004**, *108*, 5901.
(44) Bauer, P.; Wietasch, H.; Lindner, S. M.; Thelakkat, M. *Chem. Mater.* **2007**, *19*, 88.
(45) Macneill, C. R.; Abrusci, A.; Zaumseil, J.; Wilson, R.; Maxkiernan, M. J.; Burroughes, J. H.; Halls, J. M.; Neil, C.; Friend, R. *Appl. Phys. Lett.* **2007**, *90*, 193506.
(46) Edda, E. N.; Stefan, C. J.; Pual, A.; Jeroen, K. J.; Meijer, E. W.; Rene, A. J.; Dupin, H.; Geoffrey, P.; Jerome, C.; Roberto, L.; Bredas, J.-L.; David, B. *J. Am. Chem. Soc.* **2003**, *125*, 8625.
(47) Shen, D. Y.; Venkatesh, G. M.; Burchell, D. J.; Shu, P. H.; Hsu, S. L. *J. Polym. Sci. Polym. Phys. Ed.* **1982**, *20*, 509.
(48) Wang, S.; Wu, P.; Han, Z. *Macromolecules* **2003**, *36*, 4567.
(49) Jancy, B.; Asha, S. K. *Chem. Mater.* **2008**, *20*, 169.
(50) Osaheni, J. A.; Jenekhe, S. A. *Macromolecules* **1994**, *27*, 739.
(51) Lee, S. K.; Zu, Y.; Herrmann, A.; Geerts, Y.; Mullen, K.; Bard, A. J. *J. Am. Chem. Soc.* **1999**, *121*, 3513.
(52) Osaheni, J. A.; Jenekhe, S. A. *Chem. Mater.* **1995**, *7*, 672.
(53) Sandanaraj, B. S.; Robert, D.; Thayumanavan, S. *J. Am. Chem. Soc.* **2007**, *129*, 3506.
(54) Narayan, K. S.; Alagiriswamy, A. A.; Spry, R. J. *Phys. Rev. B* **1999**, *59*, 10054.
(55) Singh, Th. B.; Erten, S.; Gunes, S.; Zafer, C.; Turkmen, G.; Kuban, B.; Teoman, Y.; Sariciftci, N. S.; Icli, S. *Org. Electron.* **2006**, *7*, 480.
(56) Kohlman, R. S.; Epstein, A. J. In *Handbook of Conducting Polymers*, 2nd ed.; Skotheim, T. ; Elsenbaumer, R.; Reynolds, J., Eds.; Marcel Dekker: New York, 1998.
(57) Narayan, K. S.; Kumar, N. *Appl. Phys. Lett.* **2001**, *79*, 1891.

JP107232U